STM JOURNALS

International Journal of
Mineral

https://journals.stmjournals.com/ijmi.

Volume 3, Issue 1, 2026.
January—June.
DOI (Journal): 10.37591/IJMI.

Review IJMI

Iron Ore Beneficiation through Reverse Flotation: Advances in Nanobubble-Assisted Flotation Technology for Lean Grade Ore Upgradation and Silica Removal: A Review

Mihir D.M.[1,*], Attel Umasanka[2]

Abstract

The global demand for high-grade iron ore concentrates continues to surge as readily available rich ores become depleted. Iron ore beneficiation through froth flotation has emerged as a critical technology for upgrading lean-grade iron ores (typically 25–35% Fe) to produce high-quality concentrates (64–70% Fe) suitable for direct reduction and blast furnace operations. This comprehensive review examines the fundamental principles of flotation in iron ore beneficiation, with particular emphasis on the revolutionary impact of nanobubble (NB) assisted flotation technology. Nanobubbles, ultrafine bubbles with diameters ranging from 300 to 700 nm, offer unprecedented advantages in enhancing flotation kinetics, collector adsorption efficiency, and mineral selectivity for the separation of fine and ultrafine particles. This paper synthesizes the current state of the art in nanobubble generation via hydrodynamic cavitation, the mechanisms of nanobubble-enhanced flotation, surface chemistry fundamentals, and the critical role of reverse flotation (cationic and anionic) in silica removal from lean iron ores. Industrial case studies from global operations, process intensification strategies, and comparative analyses of nanobubble versus conventional flotation demonstrate improvements in iron recovery (20 to 40 percentage points), flotation rate acceleration (30 to 50%), and a significant reduction in reagent consumption. The paper addresses current challenges in processing Anshan-type ores and other refractory hematite deposits, discusses scale-up considerations, and projects future research directions in nanobubble-assisted flotation for sustainable iron ore beneficiation.

Keywords: Iron ore, flotation, nanobubbles, hydrodynamic cavitation, silica removal, lean grade ores, reverse flotation, surface chemistry, collector adsorption, mineral processing

INTRODUCTION

*Author for Correspondence
Mihir D.M
E-mail: mihir.dm@jsw.in

[1]AGM, BHQ Operations, R&D, JSW Steel, Vijayanagar works, Toranagallu, Bellary, Karnataka, India.
[2]Head BHQ Projects, JSW Steel, Vijayanagar works, Toranagallu, Bellary, Karnataka, India.

Received Date: December 27, 2025
Accepted Date: January 20, 2026
Published Date: January 31, 2026

Citation: Mihir D.M., Attel Umasanka. Iron Ore Beneficiation through Reverse Flotation: Advances in Nanobubble-Assisted Flotation Technology for Lean Grade Ore Upgradation and Silica Removal: A Review. International Journal of Mineral. 2026; 3(1): 1–30p.

Global Iron Ore Resources and Beneficiation Challenges

The global iron ore industry faces unprecedented challenges as the quality of exploitable reserves continues to deteriorate. According to the U.S. Geological Survey, approximately 170 billion tons of iron ore reserves exist globally, representing 83 billion tons of contained metallic iron [1]. However, the distribution is highly uneven, with Australia (29.4%), Russia (14.7%), Brazil (13.5%), and China (12.4%) holding the largest reserves [1]. Critically, while Russia and Brazil possess relatively high-grade ores (>65% Fe), China the world's largest iron ore producer and consumer must contend with predominantly low-grade deposits averaging 30–35% Fe [2].

The intensifying depletion of high-grade ore reserves globally has necessitated the processing of increasingly difficult and low-grade ore types. This shift presents substantial technical and economic challenges: conventional methods such as gravity separation and magnetic separation, while effective for coarse-grained liberation, become progressively less effective as liberation size decreases below 150 μm [3, 4]. Consequently, fine and ultrafine fractions now constituting 50–80% of run-of-mine material in many operations are increasingly processed through flotation, the only economically viable technology for this size range [5].

The Iron Ore Flotation Landscape

Froth flotation, fundamentally a surface-selective separation process exploiting differences in mineral hydrophobicity, has been the primary technique for upgrading non-magnetic iron ores and completing the separation of magnetic ores since its industrial adoption in the 1930s [1, 6]. The process operates by rendering the target mineral (iron oxide) hydrophobic through reagent adsorption while keeping gangue minerals (primarily silica) hydrophilic. Air bubbles selectively collect the hydrophobized particles, transporting them to the froth overflow as concentrate, while hydrophilic material remains as tailings [3, 4].

Despite nearly a century of industrial refinement, conventional flotation remains fundamentally limited when processing ultrafine (sub-45 μm) and microfine (sub-20 μm) fractions due to:

1. *Particle entrainment:* Hydrophilic fine particles are mechanically swept into the froth without selective attachment to bubbles [2, 7].
2. *Bubble particle interaction:* Conventional bubbles (250–500 μm) present low collision probability with fine particles due to hydrodynamic bypass effects [8].
3. *Slime coating:* Ultrafine slimes (typically <10 μm) coat coarser particles, masking their natural flotation characteristics and requiring energy-intensive desliming operations [1, 9].
4. *Reagent efficiency:* Conventional flotation exhibits lower collector adsorption rates on fine particle surfaces due to unfavorable electrostatic interactions and weak hydrophobic attraction [10].

Emergence of Nanobubble Technology

The introduction of nanobubbles bubbles with diameters in the range of 300–700 nm (0.3–0.7 μm) generated through hydrodynamic cavitation represents a paradigm shift in flotation technology [11, 12]. Unlike conventional bubbles that rise rapidly due to buoyancy, nanobubbles exhibit unique properties that fundamentally alter flotation physics and chemistry:

- *Large contact angles:* Surface nanobubbles exhibit contact angles exceeding 150°, dramatically larger than those of conventional bubbles (~90°) [13].
- *Long residence time:* Reduced buoyancy allows nanobubbles to remain in the pulp much longer, increasing collision probability with fine particles [14].
- *Surface nucleation:* Nanobubbles preferentially form and persist on hydrophobic particle surfaces, creating sites for secondary bubble attachment [11, 15].
- *Electrostatic effects:* Nanobubbles reduce electrostatic repulsion between particles and between particles and collectors, enhancing adsorption and promoting agglomeration [16, 17].

Recent innovations in nanobubble generation via hydrodynamic cavitation including various reactor designs (orifice plates, Venturi tubes, ultrasonic systems) have made this technology increasingly accessible for industrial scale-up [18, 19]. Published studies demonstrate that nanobubble-assisted flotation improves graphite recovery by 14.7 percentage points, increases coal flotation recovery by 20–27%, and enhances flotation kinetics by 30–50% [20, 21].

Objectives and Scope

This review comprehensively examines:

1. Fundamental principles of froth flotation applied to iron ore beneficiation.

2. Surface chemistry governing iron mineral reagent interactions and silica selectivity.
3. Working principles and reactor configurations for nanobubble generation.
4. Mechanisms by which nanobubbles enhance flotation efficiency.
5. The role of reverse flotation (cationic and anionic) in lean ore upgrading.
6. Desliming strategies enabling effective flotation.
7. Industrial applications and case studies across major iron ore producing regions.
8. Comparative performance: nanobubble versus conventional flotation.
9. Challenges in processing refractory ores (Anshan-type, carbonate-bearing deposits).
10. Future directions in nanobubble-assisted flotation and process intensification.

FUNDAMENTALS OF FROTH FLOTATION IN IRON ORE BENEFICIATION

Flotation as a Surface-Selective Separation Process

Froth flotation operates on the principle of exploiting hydrophobic-hydrophilic differences between minerals to achieve physical separation [1, 22]. The process relies on four essential components:

Mineral Particles

In iron ore, the valuable minerals include hematite (Fe_2O_3), magnetite (Fe_3O_4), and goethite ($FeO \cdot OH$), while gangue consists primarily of silica (SiO_2), quartz, and silicate minerals [1, 2].

Bubbles

Air bubbles (in conventional flotation: 250–5000 μm; in nanobubble flotation: 100–700 nm) serve as collectors of hydrophobic particles [23].

Reagents

Chemical additives selectively modify mineral surface properties:

- *Collectors:* Render target minerals hydrophobic through adsorption.
- *Depressants:* Maintain gangue minerals in hydrophilic state.
- *Activators:* Enhance target mineral flotability through surface modification.
- *Frothers:* Stabilize bubble structure and froth layer.

Pulp

An aqueous slurry (typically 20–35% solids by weight) in which minerals are suspended [1, 4] (Figure 1).

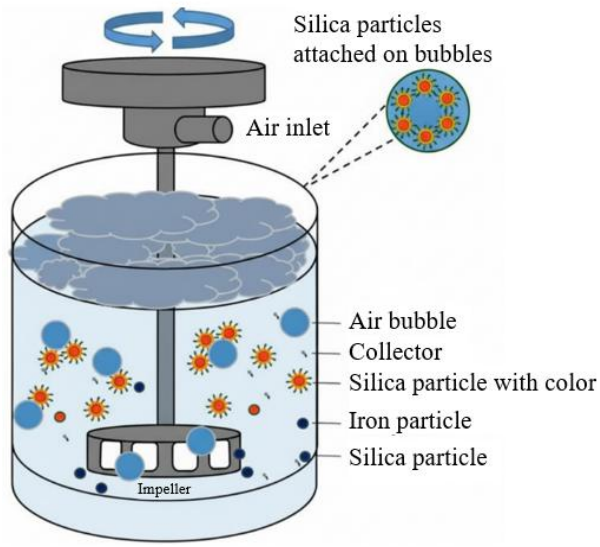

Figure 1. Schematic image of iron ore reverse flotation.

Thermodynamic and Kinetic Considerations

Flotation success depends on minimizing the Gibbs free energy of mineral-bubble interaction (Figure 2). The three-phase contact angle (θ) measured through the liquid phase between the gas and mineral surfaces directly correlates with flotation probability:

Where γ represents interfacial tensions between solid-mineral (SM), liquid-mineral (LM), and solid-liquid (SL) interfaces [3, 22].

Particles with contact angles approaching 180° (highly hydrophobic) attach readily to bubbles and float; contact angles near 0° (hydrophilic) are rejected. Iron oxides naturally possess contact angles of 5–30° (hydrophilic), requiring collector adsorption to achieve flotation angles of 60–90° [24]. Silica surfaces remain hydrophilic even at high pH, essential for their rejection in reverse flotation [3].
Flotation kinetics follow first-order rate equations:

$$R_t = R_\infty(1 - e^{-kt})$$

Where R_t is recovery at time t, R_∞ is ultimate recovery, and k is the flotation rate constant [20]. Increased bubble surface area and improved particle-bubble interaction kinetics through nanobubble technology directly enhance k values [8].

Zeta Potential and Surface Charge

The zeta potential (ζ) the electric potential at the mineral surface relative to the bulk liquid critically governs:

1. *Electrostatic interactions between particles:* Minerals with identical surface charge exhibit electrostatic repulsion, promoting dispersion; opposite charges promote flocculation.
2. *Collector adsorption:* Anionic collectors adsorb electrostatically on positively charged mineral surfaces; cationic collectors require negative surfaces.
3. *Effectiveness of depressants:* Depressants stabilize electrostatic repulsion, maintaining particle dispersion and preventing flotation.

For hematite (point of zero charge, PZC ≈ 6.5–8.5), zeta potential becomes increasingly negative at alkaline pH values typical in flotation (pH 9–12) [1, 25]. For silica (PZC ≈ 2.5–3), zeta potential is highly negative across all practical flotation pH values, enabling selective separation through pH manipulation [1].

Nanobubbles, by reducing zeta potential magnitude through surface adsorption, reduce electrostatic repulsion and promote beneficial particle agglomeration as a critical advantage in processing fine fractions [16, 17] (Figure 3).

$$\cos(\theta) = \frac{\gamma_{SM} - \gamma_{LM}}{\gamma_{SL}}$$

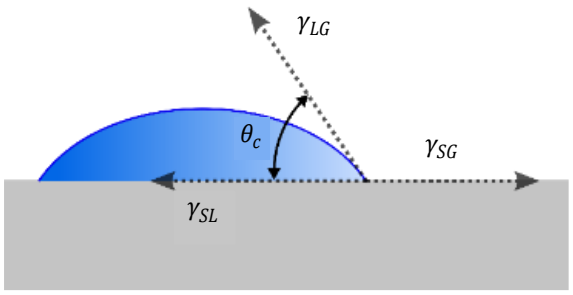

Figure 2. Schematic of contact angle.

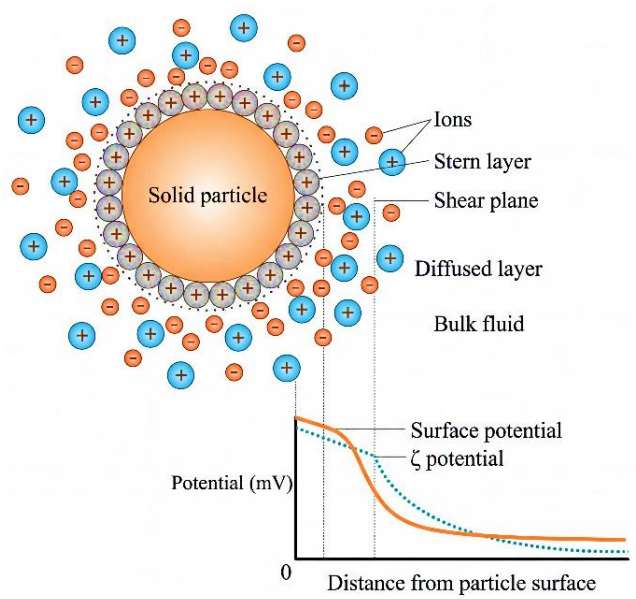

Figure 3. Schematic illustration of electrical double layer.

Particle Size Effects on Flotation Efficiency

Flotation efficiency exhibits a complex relationship with particle size [1, 7, 26]

- *Optimal range (10–100 μm):* Particles in this range exhibit highest flotation rates and selectivity. Sufficient mass enables efficient bubble attachment; manageable surface area prevents excessive slime effects.
- *Fine particles (1–10 μm):* These particles exhibit significantly reduced flotation due to its low mass which reduced settling rates and easy hydrodynamic bypass around bubbles, high surface area which disproportionate consumption of costly reagents. Entrainment susceptibility in which hydrophilic fines mechanically carried to froth despite poor collector attachment.
- *Ultrafine particles (<1 μm):* Classical flotation is largely ineffective; particles follow slurry flow patterns rather than attaching to bubbles.
- *Coarse particles (>100 μm):* Liberation decreases, and particles may be too massive for bubble support in low-density froth [1, 7]. However, coarse unliberated particles containing both iron mineral and silica present challenges requiring novel approaches.

Nanobubbles address fine particle flotation through multiple mechanisms: (1) reduced bubble size enables collision with fine particles previously missed by large bubbles, (2) surface nanobubbles promote hydrophobic agglomeration, increasing effective particle size, and (3) enhanced collector adsorption at nanobubble-particle interfaces [11, 20, 21].

IRON ORE FLOTATION ROUTES AND PROCESSING STRATEGIES

Direct Flotation

Direct flotation floats iron minerals into the froth product while rejecting gangue to tailings. This approach is operationally simpler requiring fewer reagent types but has been largely supplanted by reverse flotation in modern operations due to fundamental limitations [1].

Alkaline Medium Direct Flotation (pH 9–10)

- *Collector:* Fatty acids (oleic, linoleic acids; ~91% saponified material).
- *Mechanism:* Fatty acid anions adsorb on iron mineral surfaces.
- *Advantage:* Simple, low reagent cost, effective without desliming.
- *Disadvantage:* High-grade separation difficult due to similar zeta potentials of iron oxides and silicates at alkaline pH; limited to iron grades <64%.

Weakly Acidic Medium Direct Flotation (pH 5.5–7)

- *Collector:* Sodium petroleum sulfonate, fatty acids.
- *Mechanism:* Increased zeta potential differentiation between minerals enables better separation.
- *Advantage:* Achieves higher iron grades (up to 63.6% from 28.94% feed).
- *Disadvantage:* Highly sensitive to slime content due to hetero-coagulation; requires intensive desliming; higher filtration difficulties.

Currently direct flotation has been largely replaced globally due to superior performance of reverse flotation, now accounting for >90% of industrial flotation circuits [1].

Reverse Cationic Flotation

Reverse cationic flotation, the dominant technology for iron ore beneficiation in the Americas, Brazil, India, and portions of Russia, floats silica gangue to reject it while concentrating iron minerals in tailings that are thickened or filtered [1, 27].

Mechanism and Chemistry

- *Collector:* Primary and secondary ether amines (e.g., unneutralized primary ether amine, alkyl ether monoamines)
- *Depressant:* Corn starch or other polysaccharides
- *pH range:* 9.5–10.5 (alkaline conditions)
- *Operating principle:* Silica surfaces, being naturally negatively charged at all practical pH values, are activated by adsorption of cationic amine collector molecules:

$$\text{R-NH}_2 + \text{SiO}_2^- \rightarrow \text{R-NH}_3^+ \cdots \text{SiO}_2^-.$$

The adsorbed amine layer renders silica hydrophobic, enabling flotation. Iron oxides, which are positively charged in this pH range, are depressed through starch adsorption:

$$\text{Starch-OH} + \text{Fe}^{3+}/\text{Fe}^{2+} \rightarrow \text{Starch-O-Fe complex}$$

This complex creates a hydrophilic film preventing collector adsorption [1].

Industrial Applications and Performance

- *Tilden Mine (Michigan, USA):* Processes low-grade hematite ore (after grinding to 80% passing 25 μm) through multi-stage desliming followed by reverse cationic flotation with secondary ether amine collector. Final concentrate: 64–67% Fe, ~5% SiO_2, 75% Fe recovery [1] (Figure 4).
- *Empire Mine (Michigan, USA):* Processes magnetite concentrate (prepared by 2-stage magnetic separation) at 63% Fe initial grade. Flotation with amine collector (ADMAG-83) removes residual silica, achieving final concentrate of 69% Fe, <3.5% SiO_2, with 96% flotation recovery [1].
- *Samarco Mine (Brazil):* Processes 53% Fe hematite ore, achieving 15.5 million tons/year crude concentrate at 67.17% Fe, 1.1% SiO_2 [1].
- *Sept-Îles (Canada):* Flotation circuit with 8 rougher, 3 cleaner, and 8 total scavenger cells produces concentrate at 64% Fe, 4.5% SiO_2, 93.5% Fe recovery [1].

Advantages and Disadvantages

Advantages

1. High flotation rates enabling short residence times.
2. Operational simplicity and ease of control.
3. Synergistic effects with preceding magnetic separation.
4. Proven technology at global industrial scale.

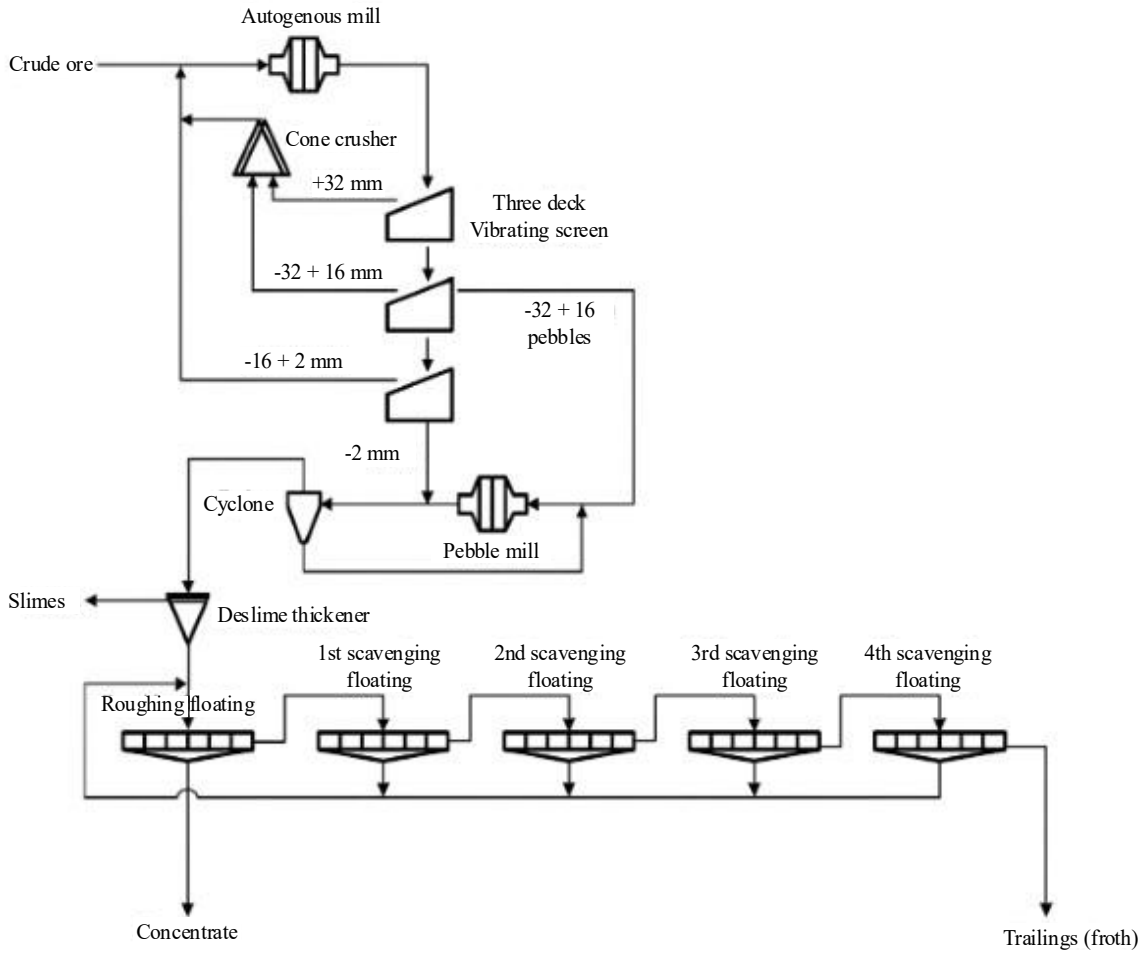

Figure 4. Overview of the Tilden Mine iron ore beneficiation process, utilizing cationic reverse flotation (based on Houot 1983).

Disadvantages

1. Complex adsorption behavior of amine collectors; selectivity often lower than anionic collectors.
2. Many amine collectors exhibit significant frother properties, resulting in viscous, stable froth difficult to drain – poor selectivity.
3. Collector toxicity requiring environmental management.
4. Amine collector cost and availability (historically limited in some regions) [1, 28].

.

Reverse Anionic Flotation

Reverse anionic flotation, pioneered in China and increasingly applied globally, uses anionic collectors (fatty acids) to float silica after activation with divalent cations (Ca^{2+}, Mg^{2+}). Iron minerals are depressed through starch at highly alkaline pH [1].

Mechanism and Chemistry

- *Collector:* Fatty acids (tall oil, oleic acid, modified collectors such as RA-315, RA-715, KS-VI, MH).
- *Activator:* Lime (CaO) providing Ca^{2+} ions.
- *Depressant:* Corn starch.
- *pH range:* 11.0–12.5 (highly alkaline).
- *Operating principle:* Silica surfaces, naturally negative due to dissociation of silanol groups (-SiOH → $-SiO^- + H^+$), are activated by specific adsorption of Ca^{2+} at high pH:

$SiO^- + Ca^{2+} \rightarrow SiO\text{-}Ca^+$

The positively charged surface enables anionic collector adsorption:

$R\text{-}COO^- + SiO\text{-}Ca^+ \rightarrow R\text{-}COO.Ca.SiO$

Iron oxide surfaces, intensely negative at pH 11–12.5 ($\zeta \approx -40$ mV), are effectively depressed through strong starch adsorption via hydroxyl-metal oxide interactions [1, 25, 29].

Industrial Applications

- *Qidashan Concentrator (China):* Transitions from alkaline direct flotation (achieving 59.5% Fe) to weakly acidic direct flotation with anionic collector, eventually adopting anionic reverse flotation to achieve 67.67% Fe from 29.16% Fe feed with 71.65% recovery [1].
- *Yuanjiacun Concentrator (Tai Steel, China):* World's largest iron ore concentrator (22 million tons/year), processes ultra-fine Anshan-type hematite ore (liberation size 90% passing 45 μm) through grinding, magnetic separation, and anionic reverse flotation. Achieves 66.95% Fe concentrate, 72.62% recovery from 31.72% Fe feed ore [1].
- *Qidong Mine (Hunan, China):* Addresses extreme ultrafine liberation (95% passing 37 μm) through multi-stage grinding and selective flocculation desliming followed by anionic reverse flotation. Capacity: 3 million tons/year, target: 63–65% Fe, 65–70% Fe recovery [1] (Figure 5).
- *Anshan concentrators (China):* Multiple facilities including Gongchangling, Sijiaying, utilizing anionic reverse flotation on Anshan-type ores achieve 66–68% Fe from 28–30% Fe feed with 75–82% recovery [1].

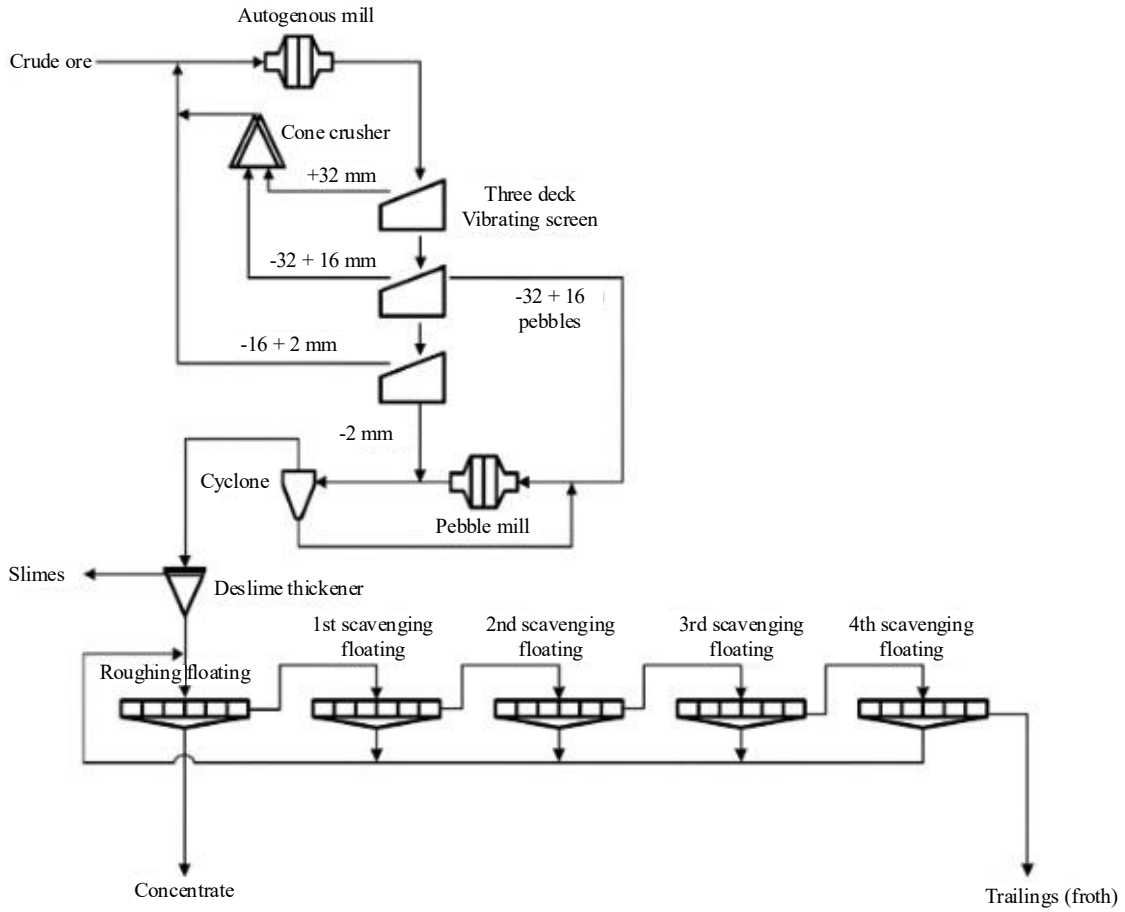

Figure 5. The Qidong concentrator uses multiple deslime and regrinding stages to separate an ultra-fine iron ore with anionic reverse flotation (based on Hu, Zheng and Xiao 2010; Liu 2003).

Advantages and Disadvantages

Advantages

1. Superior selectivity through specific activation mechanism.
2. Lower collector cost (fatty acids are paper industry waste products).
3. Decreased slime sensitivity compared to cationic flotation.
4. Excellent adaptability to mineralogical variations (particularly silicate minerals).
5. Proven effectiveness on most difficult refractory ores globally.

Disadvantages

1. Requires precise pH control (±0.5 pH units) to maintain both activation and iron depression.
2. Higher reagent consumption due to lime addition and elevated pH operation.
3. Potential scaling issues if water contains interfering ions.
4. More complex reagent systems compared to simpler alkaline direct flotation [1, 29].

Stepped Flotation for Carbonate-Bearing Iron Ores

Stepped flotation addresses the unique challenge of carbonate-bearing iron ores (containing siderite, $FeCO_3$), particularly prevalent in China's reserves (up to 5 billion tons). These ores present exceptional difficulties because siderite exhibits intermediate flotability, generating fine slimes during grinding that coat both hematite and silica, preventing effective separation through either direct or reverse flotation alone [1, 30].

Process Scheme

1. *Stage 1 (Neutral direct flotation):* Float siderite using anionic collector at pH 7–8, depress hematite with starch.
2. *Stage 2 (Anionic reverse flotation):* Float remaining silica at pH 11.5 using lime activation and fatty acid collector, depress hematite with starch.

Industrial Example

Donganshan Concentrator: Achieves concentrate of 63.02% Fe with 63.77% overall recovery through stepped flotation of siderite-bearing ore [1].

This innovative approach demonstrates the importance of understanding mineralogy and adapting flotation sequences accordingly.

DESLIMING: CRITICAL PRE-REQUISITE FOR EFFECTIVE FLOTATION

The Slime Problem in Iron Ore Flotation

Slimes particles typically <20 μm and specifically <10 μm in size present a critical problem in flotation of ground iron ores, particularly in reverse flotation operations [1, 31].

Mechanisms of Slime Interference

1. *Heterocoagulation:* Slimes with opposite charge to bulk mineral particles electrostatically adhere to coarser particles, coating them with a hydrophilic film that masks the particles' true flotation characteristics [1, 32].
2. *Particle entrainment:* Ultrafine slimes, having low mass and large surface area, are mechanically swept into the froth product without selective bubble attachment, reducing concentrate grade and requiring multiple cleaner stages.
3. *Reagent consumption:* Fine particles exhibit disproportionately large surface areas; a 1 μm particle has 100× the surface area per unit mass of a 10 μm particle. Slimes may consume 30–60% of collector dosage despite comprising only 10–20% of mass [1, 31].
4. *Bubble surface occlusion:* Ultrafine particles may adsorb to bubble surfaces without beneficial orientation, occupying active collection sites that should be reserved for coarser valuable particles [1, 32].

5. *Industrial evidence:* At Mikhailovsky plant (Russia), removal of sub-10 μm particles from wet magnetic separation tailings resulted in improved selectivity, indicating that the presence of fine slimes actively degrades flotation performance [1].

Conventional Desliming Methods

Cyclone

- *Operates on settling differential;* separation efficiency depends on particle density, size, and cyclone geometry
- *Typical cut size:* 20 μm for iron ore applications.
- *Industrial example:* Tilden Mine utilizes two desliming stages with cyclones; deslime overflow accounts for 15–30% total material loss and 5% iron loss [1].
- *Advantage:* Simple, robust, low operating cost.
- *Disadvantage:* Limited cut size flexibility; material loss of valuable iron-bearing slimes.

Thickeners

- Gravity settling with adjustable rise rate to achieve desired cut size.
- Can achieve finer cut sizes than cyclones.
- *Disadvantage:* Large footprint, slow operation, high capital cost.

High-Gradient Magnetic Separators (HGMS)

- Removes ultrafine magnetically susceptible particles (magnetite, some iron minerals).
- Limited effectiveness for non-magnetic materials.
- May not effectively remove non-magnetic slimes [1].

Selective Flocculation Desliming

Selective flocculation has emerged as the preferred industrial desliming methodology, particularly for alkaline flotation operations. The technique exploits electrostatic differences between minerals to achieve selective aggregation of target minerals while maintaining fine gangue dispersed [1, 31].

Selective Flocculation Principle

1. *Dispersion stage:* Sodium silicate or sodium polyacrylate dispersants at alkaline pH (9–10) create repulsive electrostatic forces between fine particles.
2. *Flocculation stage:* Corn starch addition preferentially flocculates iron-bearing minerals (hematite, magnetite) while maintaining silicate and silica particles dispersed.
3. *Separation:* Flocculated iron minerals settle while ultrafine slimes remain suspended and are discarded as overflow.

Chemistry of Selective Flocculation

- Starch contains hydroxyl groups that form hydrogen bonds with hydroxylated mineral surfaces.
- Iron minerals, with surface -OH groups, form strong starch complexes.
- Silica, lacking reactive hydroxyl sites, shows minimal starch interaction.
- Divalent cations (Ca^{2+}, Mg^{2+}) if present may promote unwanted heterocoagulation [1, 31, 33].

Industrial Implementation

- *Tilden Mine:* Two-stage selective flocculation using sodium hydroxide dispersion followed by corn starch flocculation in deslime thickener; achieves deslime underflow of ~44% Fe grade [1].
- *Yuanjiacun Concentrator:* Multi-stage grinding with selective flocculation desliming enables processing of ultra-fine ores [1].
- *Qidong Mine:* Multiple desliming and grinding stages with selective flocculation achieve target grades on ultra-fine, difficult ores [1].

- *Recent Advances:* Addition of polyacrylamide and polyacrylate dispersants (in place of traditional sodium silicate) has improved performance and reduced water hardness sensitivity in recent industrial trials [1].

SURFACE CHEMISTRY AND MINERAL-REAGENT INTERACTIONS

Iron Oxide Surface Properties

Iron minerals in flotation – primarily hematite (Fe_2O_3) and magnetite (Fe_3O_4) – exhibit complex surface chemistry governed by hydration, oxidation state, and pH-dependent hydroxylation [1, 25, 34].

Hematite Surface Chemistry

Hematite surface in aqueous solution is characterized by:

Surface hydroxylation

$$Fe\text{-}O^{2-} + H_2O \rightleftharpoons Fe\text{-}OH^{+} \text{ or } Fe\text{-}OH^{-}$$

pH-Dependent Behavior

- *Acidic pH (<6):* Surface exhibits positive charge; $-OH^-$ groups accept protons → $Fe\text{-}OH_2^+$, rendering surface hydrophilic
- *Neutral pH (6–8):* Mixed surface charge; PZC ≈ 6.5–8.5 depending on iron oxidation state and surface roughness
- *Alkaline pH (>9):* Surface becomes increasingly negative through deprotonation of water → $Fe\text{-}O^-$, achieving highly negative zeta potential (~-40 mV at pH 11) [1, 25] (Figure 6).

Implications for Flotation

- At alkaline pH typical in reverse flotation, hematite is naturally rendered hydrophilic, enabling effective depression through starch or other depressants.
- Amine collectors (cationic) cannot effectively adsorb on negative hematite surfaces through electrostatic mechanisms, requiring starch depression to prevent unwanted flotation.
- Anionic collectors similarly find hematite surfaces unfavorable, enabling selective flotation of activated silica [1].

Magnetite Surface Chemistry

Magnetite (Fe_3O_4), containing mixed Fe^{2+}/Fe^{3+}, exhibits more complex surface chemistry:

- *Higher floatability at lower pH:* Fe^{2+} on surface may be oxidized or reduced depending on oxygen availability.
- *More hydrophobic than hematite naturally:* May float without collector under certain conditions.
- *Dual functionality:* Can be depressed at alkaline pH through mechanisms similar to hematite (depressants), enabling separation from silica through reverse flotation [1, 27].

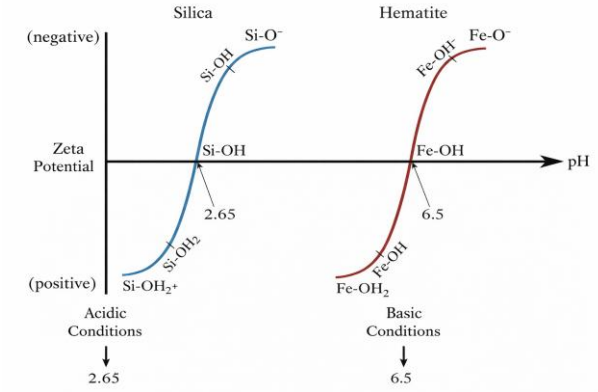

Figure 6. Schematic response of zeta potential to pH changes for the hematite and silica (quartz).

Silica Surface Chemistry

Silica (SiO_2, primarily quartz in iron ores) exhibits fundamentally different surface characteristics essential to reverse flotation success:

Surface hydroxylation

$$Si\text{-}O^- + H^+ \rightleftharpoons Si\text{-}OH$$

pH-Dependent Behavior

1. *Entire practical pH range (0–14):* Silica surface remains highly negative due to very low PZC (~2–3).
2. *Alkaline pH (>5):* Zeta potential: highly negative (~-50 to -70 mV), maintaining hydrophilicity.
3. *Neutral to slightly acidic pH:* Still predominantly negative, maintaining hydrophilicity [1, 25].

Critical Observation

Silica cannot be rendered hydrophobic at practical pH values through simple pH manipulation. Instead, activation through divalent cation adsorption (Ca^{2+} via lime in anionic reverse flotation; dual mechanisms in cationic reverse flotation) is required [1].

Collectors and Adsorption Mechanisms

Anionic Collectors (Fatty Acids)

- *Structure:* Long aliphatic hydrocarbon chains with terminal carboxyl group (-COOH).
- *Examples:* Oleic acid, linoleic acid, tall oil (mixture of C_{16}-C_{18} fatty acids), modified collectors (RA-series, MH, KS-VI).

.

Adsorption on Activated Silica

1. At high pH (11–12), carboxyl group ionizes: $R\text{-}COOH \rightarrow R\text{-}COO^-$
2. Anionic carboxylate anions adsorb physically on positively charged, Ca^{2+}-activated silica surfaces.
3. Hydrophobic alkyl chains orient toward aqueous phase, rendering surface hydrophobic [1, 29, 35].

Adsorption on Hematite

- Due to highly negative hematite surface at alkaline pH, anionic collector adsorption is minimal.
- Depression is enhanced by starch, which through hydrogen bonding and metal-oxide interactions creates an additional hydrophilic layer [1].

Advantages

- Natural waste products from paper/soap industries → low cost.
- Superior selectivity for silica activation.
- Lower sensitivity to slime coatings at high pH [1].

Cationic Collectors (Amines)

- *Structure:* Aliphatic or aromatic chains with terminal amino group ($-NH_2$).
- *Examples:* Primary ether amines, secondary amines, alkyl ether monoamines (EBAB).

Adsorption on Silica

1. Amine group ionizes at alkaline pH: $R\text{-}NH_2 \rightleftharpoons R\text{-}NH_3^+$ (weak, dependent on amine type).
2. Cationic amine adsorbs electrostatically on negative silica surface.
3. Hydrophobic alkyl chains orient toward gas phase, enhancing flotation [1, 27]

Limitations

1. Many amine collectors exhibit inherent frother properties, producing excessive, unstable froth.
2. Complex adsorption behavior; selectivity often compromised.
3. Toxicity concerns; environmental hazard if improperly managed.
4. Regional availability issues in some locations (historically limited in China) [1, 28].

Depressants

Starch (primary choice)

- Polysaccharide with abundant hydroxyl (-OH) groups.
- Forms strong hydrogen bonds and metal-oxide complexes with iron mineral hydroxylated surfaces.
- *Mechanism:* Multiple -OH groups across starch polymer enable formation of bridging complexes between starch and surface Fe^{3+}/Fe^{2+}:.
- Fe-OH + Starch-OH → Fe.O-Starch (hydrogen bond/coordination complex).
- *Dosage:* Typically, 0.5–2.0 kg/ton of ore.
- Effectiveness increases at high pH (optimal at pH 11–12) due to increased surface hydroxylation [1, 29, 33].

Alternative depressants

- *Dextrin (modified starch):* Enhanced performance reported in some operations [1].
- *Carboxymethyl cellulose (CMC):* Effective for specific ore types.
- *Sodium silicate:* Primarily used as dispersant in desliming, also provides weak depression [1].

Activators and Surface Modification

Lime (CaO) in Anionic Reverse Flotation

1. *Dissolution in pulp:* $CaO + H_2O \rightarrow Ca(OH)_2$
2. Ca^{2+} ions specifically adsorb on silica surface.
3. *Surface charge reversal:* Negative silica surface (SiO^-) becomes positively charged through cation adsorption:

$$SiO^- + Ca^{2+} \rightarrow >SiO\text{-}Ca^+$$

4. Positive surface enables anionic collector (fatty acid) adsorption.
5. *Dosage:* Typically, 0.3–1.0 kg/ton to achieve desired pH and activation [1, 29].

Dual Role of Lime

- *Chemical:* Activates silica through Ca^{2+} adsorption.
- *pH buffering:* Maintains alkaline pH necessary for iron oxide depression and starch effectiveness [1].

NANOBUBBLES: GENERATION, CHARACTERIZATION, AND FUNDAMENTALS

Definition and Key Characteristics

Nanobubbles (NBs) are ultrafine gas bubbles with diameters typically in the range of 100–1000 nm, though the practical range for flotation applications is 300–700 nm [11, 12, 36]. They represent a distinct class of bubble intermediate between molecular solutions and conventional microbubbles [37] (Table 1).

Physical Characterization Techniques

1. *Nanoparticle Tracking Analysis (NTA):* Measures bubble size distribution (30–1000 nm range) and concentration through light scattering and Brownian motion tracking [38].
1. *Atomic Force Microscopy (AFM):* Enables direct visualization of surface nanobubbles on mineral particle surfaces; reveals contact angles and morphology [13, 39].
2. *Transmission Electron Microscopy (TEM):* High-resolution imaging of nanobubble structure and interface characteristics [40].
3. *Dynamic Light Scattering (DLS):* Provides hydrodynamic diameter and polydispersity index [16, 38].

Table 1. Key distinguishing properties.

Property	Conventional Bubbles	Nanobubbles
Diameter	250 μm – 5 mm	100–1000 nm (typically 300–700 nm)
Surface area/volume	Low	Extremely high (100–1000× higher)
Contact angle	~90°	140–180° (highly wetting)
Rising velocity	Rapid (buoyancy-driven)	Minimal (reduced buoyancy)
Residence time in pulp	Seconds	Minutes to hours
Stability	Minutes	Hours to days (depending on conditions)
Natural occurrence	Not applicable	Ubiquitous in cavitation systems

Nanobubble Generation via Hydrodynamic Cavitation

Hydrodynamic cavitation – the formation of vapor bubbles due to pressure reduction below saturation pressure during rapid fluid flow – is the preferred industrial method for nanobubble generation due to simplicity, efficiency, and scalability [11, 18, 36].

Cavitation Mechanisms

Cavitation Inception: Occurs when local static pressure falls below vapor pressure of liquid:

$P_{\text{local}} < P_{\text{vapor}} \rightarrow$ Bubble nucleation

Bubble collapse (implosion): As flow velocity decreases and pressure recovers, bubbles collapse violently:

$\Delta P = P_{\text{collapse}} - P_{\text{recovery}} \rightarrow$ Implosive collapse

This high-energy collapse generates:

- Pressure waves (potentially >1000 MPa locally).
- Microjet streams (velocities >100 m/s).
- Local temperature spikes (>5000 K in extreme cases).
- Free radicals (OH, H) in aqueous solutions.

These extreme conditions promote bubble fragmentation and nanobubble stabilization [18, 41].

Reactor Configurations

Orifice-Plate Design

- Simple plate with drilled holes creates localized pressure reduction.
- *Advantages:* Simple construction, low cost.
- *Disadvantages:* High wear, material erosion, limited control over bubble size.
- Industrial application: Small-scale batch operations [11, 18].

Venturi Tube Design

- Converging-diverging geometry creates pressure reduction in throat.
- *Advantages:* Smooth operation, controlled cavitation, less erosion.
- *Disadvantages:* Higher pressure drop, more complex construction.
- *Industrial application:* Moderate-scale continuous operations [18, 19]

Ultrasonic Cavitation

- Acoustic waves (typically 20–100 kHz) induce cavitation
- *Advantages:* Precise control, effective nanobubble generation
- *Disadvantages:* Energy-intensive, not easily scalable to large volumes
- *Industrial application:* Laboratory and pilot-scale work [41]

Rotor-Stator Devices (Hydrodynamic Cavitation Cells)

- Rotating impeller creates shear-induced cavitation
- *Advantages:* Robust, scalable, integrable into flow streams
- *Disadvantages:* Mechanical complexity, wear considerations
- *Industrial application:* Emerging in large-scale flotation circuits [19, 42]

Cavitation Parameters Affecting Bubble Size

Research has established quantitative relationships between cavitation operating parameters and resulting nanobubble size distribution [18, 36, 43]:

Cavitation Time

- As cavitation duration increases from 0 to 15 minutes, initial large bubbles (1000 nm) fragment into stable nanobubbles
- Optimal cavitation time varies: 7–10 minutes typical for orifice-based systems; 12–15 minutes for some Venturi designs
- Extended cavitation beyond optimum shows minimal further size reduction, suggesting equilibrium distribution [16, 36]

Frother Concentration

- Frothers stabilize bubble surfaces through molecular orientation at interfaces
- Surface coverage reduces surface tension, suppressing coalescence and promoting finer bubbles
- Optimal frother concentration typically 20–50 mg/L; excess frother provides diminishing returns [16, 37, 44].

Pressure Drop (Δ P)

- Higher pressure drops across cavitation devices create more intense cavitation
- Relationship not strictly linear but generally: smaller bubbles at higher Δ P
- Practical industrial systems operate 0.3–2.0 MPa [18, 19]

Air Inlet Volume

- Adjusting air injection rate affects bubble generation efficiency.
- *Typical range:* 50–200 mL/min for laboratory-scale systems.
- Higher air volumes may increase bubble concentration but reduce stability if coupled with excessive cavitation intensity [36].

Temperature

- Elevated temperature increases vapor pressure, reducing cavitation intensity.
- Cold water (4°C) shows enhanced nanobubble generation and stability.
- Practical flotation operations accept ambient temperature constraints [36].

Nanobubble Stability and Characterization

A critical distinction separates nanobubbles from bulk (conventional) bubbles: surface nanobubbles formed on mineral particle surfaces exhibit exceptional stability (hours to days) despite violating classical physics predictions that small bubbles should rapidly dissolve [12, 43, 44].

Surface Nanobubble Stability Mechanisms

Interfacial curvature and Laplace pressure

Classical Laplace equation predicts that bubbles smaller than ~1 μm should dissolve rapidly:

$$\Delta P = \frac{2\gamma}{r}$$

For a 500 nm bubble: ΔP ≈ 300 kPa – far exceeding dissolved oxygen pressure, predicting rapid dissolution [12, 43].

Explanation for Anomalous Stability

1. *Reduced gas diffusion at contact line:* Pinning of contact line at rough surface features prevents expansion of bubble mouth, reducing gas flux into bulk solution [45].
2. *Supersaturation in confined cavity:* Hydrophobic surface traps gas at interface; gas becomes supersaturated in confined space bounded by surface and water [12].
3. *Pinned contact angle:* Nanobubbles on hydrophobic surfaces maintain large contact angles (140–180°) through geometric constraints, preventing shrinkage [13].
4. *Interfacial composition:* Impurities (organic molecules, ions) at gas-liquid interface reduce effective surface tension, affecting diffusion kinetics [44].

Bulk vs. Surface Nanobubbles

Bulk nanobubbles (in solution) are generated throughout cavitation and are dispersed uniformly within the liquid. They typically have smaller characteristic sizes (about 100–300 nm) and exhibit high stability, persisting from minutes to several hours. In contrast, surface nanobubbles (on particle surfaces) form preferentially on hydrophobic surfaces during cavitation or froth flotation operations. These nanobubbles are generally larger (approximately 300–700 nm) and are even more stable, remaining for several hours to days. Their primary role in flotation is to act as collectors by mediating particle–particle and particle–bubble interactions [11, 36, 45].

MECHANISMS OF NANOBUBBLE-ENHANCED FLOTATION

Large Contact Angle and Enhanced Hydrophobicity

The most distinctive characteristic of surface nanobubbles is their extremely large contact angle (140–180°), substantially exceeding that of conventional bubbles (~90°) [13, 37, 39].

Contact Angle Definition and Significance

Contact angle (θ) represents the angle measured through the liquid phase between gas and solid surfaces at three-phase contact line. It directly correlates with surface hydrophobicity:

- $\theta \rightarrow 0°$*:* Strongly hydrophilic (water wets surface completely).
- $\theta = 90°$*:* Intermediate hydrophilicity (conventional bubble).
- $\theta \rightarrow 180°$*:* Strongly hydrophobic (surface repels water).

Measurement

Contact angles of nanobubbles exceed those of macroscopic bubbles and can reach 170–180° [13, 46]. This larger angle indicates that nanobubble surfaces behave as more strongly hydrophobic "oily bubbles" rather than simple gas bubbles [39].

Consequences for Flotation

1. *Enhanced collector adsorption:* The hydrophobic nature of nanobubble surfaces creates attraction for oil-like collectors (fatty acids, diesel, kerosene) similar to collector adsorption on mineral surfaces. Enhanced Oil Collector adsorption at nanobubble-aqueous interfaces increases effective collector concentration in the pulp [21, 47].
2. *Reduced electrostatic repulsion:* Large contact angle suggests minimal water penetration under the nanobubble at the surface. This reduced hydration layer decreases electrostatic screening and reduces repulsion between negatively charged nanobubbles and similarly charged mineral surfaces or collectors [16, 48].
3. *Capillary forces between particles:* Nanobubbles bridging hydrophobic particles generate capillary attraction ("capillary force") that promotes particle agglomeration through:

$$F_{\text{capillary}} = 2\pi r\gamma \sin(\theta)$$

Where r is bubble radius, γ is surface tension, and θ is contact angle. Larger θ dramatically increases capillary force (approaches maximum at θ = 90°) [15, 49].

Hydrophobic Agglomeration and Particle Aggregation

Fine particles aggregated into larger flocs exhibit dramatically improved flotation probability [11, 15, 20, 50].

Mechanism

Hydrophobic agglomeration – the spontaneous aggregation of hydrophobic particles in aqueous suspension – is promoted by nanobubbles through multiple pathways:

Direct agglomeration

1. Nanobubbles preferentially form on hydrophobic mineral surfaces (due to reduced surface free energy at hydrophobic interfaces).
2. Multiple particles with surface nanobubbles approach each other.
3. Capillary bridging forces between adjacent nanobubbles exceed electrostatic repulsion between particles.
4. Particles aggregate into stable flocs [11, 15, 50].

Collector-Mediated Agglomeration

1. Nanobubbles reduce surface potential magnitude through adsorption
2. Reduced zeta potential decreases electrostatic repulsion between particles
3. Van der Waals attraction gains prominence over electrostatic repulsion
4. Collector-coated particles aggregate more readily [16, 17, 48]

Effective Particle Size Enhancement

- Agglomerates of ultrafine particles (original 10–50 nm) form larger effective particles (100–500 nm)
- These larger entities exhibit:
  - Reduced electrostatic hindrance to bubble attachment.
  - Sufficient mass for stable bubble support.
  - Reduced entrainment susceptibility.
  - Improved kinetic flotation constants [20, 21].

Experimental Evidence

Graphite flotation (Ma & Tao, 2022):[21]

- Nanobubble flotation completed in 40 seconds vs. 60 seconds for conventional flotation.
- Flotation rate constant increased 39% (1.50 min^{-1} vs. 1.08 min^{-1}).
- Recovery 7 percentage points higher at endpoint.
- Superior grade achieved throughout flotation.

.

Argentite Flotation (Yan et al., 2025) [17]

- Turbidity tests showed argentite particles in nanobubble-containing water exhibited higher turbidity (more dispersed), indicating that nanobubbles reduced particle aggregation tendency.
- However, in presence of collector (sodium diethyldithiocarbamate), nanobubble-treated samples showed reduced turbidity, indicating collector-promoted aggregation was enhanced by nanobubbles.
- Microscopic examination confirmed larger floc sizes with nanobubbles [17].

Ilmenite Flotation [32]

- Nanobubbles enhanced hydrophobic floc formation.
- Floc stability significantly improved in nanobubble system.
- Flotation rate enhancement observed across all particle size fractions tested [32].

Collector Adsorption Enhancement

Nanobubbles significantly enhance both the kinetics and equilibrium capacity of collector adsorption on mineral surfaces – a critical mechanism for improved mineralization efficiency [10, 21, 47, 51].

Diesel Adsorption on Graphite (Ma & Tao, 2022)

Detailed kinetic studies revealed mechanisms of nanobubble-enhanced adsorption:[21]

Adsorption Capacity

- *At 20 mg/L diesel concentration:* Maximum 2.08 mg/g in presence of nanobubbles vs. 1.98 mg/g without (5% improvement).
- *Time to equilibrium:* 5 minutes with nanobubbles vs. >7 minutes without.
- Comparison of 20 mg/L with nanobubbles to 30 mg/L without nanobubbles: Nanobubble effect equivalent to ~33% increase in collector concentration.

Kinetic Model Fit

Quasi-second-order kinetic model provided best fit ($R^2 = 0.9962$) to adsorption data:

$$\frac{t}{q_t} = \frac{1}{k_2 q_e^2} + \frac{t}{q_e}$$

Where $k_2 = 0.2941$ g·mg^{-1}·min^{-1} with nanobubbles, significantly elevated compared to conventional conditions [21].

Zeta potential Mechanism

- *Graphite surface zeta potential:* -70 mV (conventional) vs. -45 mV (nanobubbles).
- *Diesel droplet zeta potential:* -85 mV (conventional) vs. -55 mV (nanobubbles).
- 40–45 mV reduction in electrostatic repulsion magnitude directly enhances collector adsorption kinetics.
- Surface nanobubbles mask oxygen-containing (hydrophilic) groups on graphite, presenting a more hydrophobic interface favorable for collector adsorption [21, 48].

DDTC Adsorption on Argentite (Yan et al., 2025)

Comprehensive study of collector adsorption in nanobubble system:[17]

Adsorption Capacity

- DDTC (sodium diethyldithiocarbamate) adsorption on argentite reduced in nanobubble system compared to conventional flotation.
- However, this reduction reflects nanobubble formation of protective film on mineral surface.
- Effective DDTC availability at mineral surface for flotation actually improved through enhanced agglomeration and reduced entrainment [17].

Surface Characterization

- FTIR spectroscopy confirmed DDTC peaks (characteristic vibrations) present in conventional flotation products.
- Nanobubble samples showed additional features indicating different adsorption orientation or conformation.
- Spectroscopic evidence supports hypothesis that surface nanobubbles alter local surface structure and collector interaction geometry [17].

Reduced Electrostatic Repulsion and Enhanced Particle Interactions

Nanobubble adsorption on mineral surfaces reduces absolute zeta potential magnitude, weakening electrostatic repulsion and promoting desirable particle-particle and particle-collector interactions [16, 17, 48, 51].

Zeta Potential Reduction Mechanism

Quantitative Findings

- *Argentite in DI water:* $\zeta \approx$ -45 mV (pH 8).
- *Argentite in nanobubble-containing water:* $\zeta \approx$ -25 mV (pH 8).
- Reduction of 20 mV (~44%) directly correlates with enhanced agglomeration [17].

Physical Interpretation

Nanobubbles Adsorbed on Mineral Surfaces

1. Mask negatively charged surface sites (oxygen-containing groups, hydroxyl sites).
2. Reduce accessible surface area available for ion adsorption.
3. Create a gas-phase boundary layer reducing electrostatic field at fluid interface.
4. Effectively "shield" underlying negative surface charge [16, 17, 48].

.

Extended DLVO Theory Implications

Classic DLVO (Derjaguin-Landau-Verwey-Overbeek) colloidal stability theory identifies:

- *Electrostatic Repulsion:* $\propto$ (zeta potential) $^2 \rightarrow$ Reduced with nanobubbles.
- *Van der Waals Attraction:* Remains unchanged.
- *Net Interaction:* Shifts toward aggregation as repulsion decreases [48, 51].

.

Synergistic Interaction with Flotation Reagents

Nanobubbles do not merely passively enhance flotation – they actively interact with collectors, depressants, and frothers in ways that amplify overall system performance [10, 21, 47].

Collector-Nanobubble Synergy

Oil-based collectors (diesel, kerosene, fatty acids)

1. Nanobubbles form at oil-water interface due to reduced interfacial energy.
2. Oil-coated nanobubbles become "oily" secondary collectors.
3. Enhanced contact angle and hydrophobicity of nanobubble surface promote collector micelle formation.
4. Collector concentration effectively increased through nanobubble association [21, 47].

Amine-Based Collectors

1. Cationic amine collectors in alkaline solution partially ionize: $R\text{-}NH_2 \rightleftharpoons R\text{-}NH_3^+$.
2. Nanobubbles reduce electrostatic screening, enhancing interaction with collector cations.
3. Nanobubble-collector complexes more effectively adsorb on mineral surfaces [16].

Depressant Effectiveness

Depressants (starch) show enhanced effectiveness in nanobubble systems: [16, 17, 48].

1. Reduced surface electrostatic repulsion promotes depressant polymer spreading on mineral surface.
2. Enhanced hydrogen bonding between depressant and surface hydroxyl groups.
3. More complete coverage preventing collector adsorption on depressed minerals [1, 29, 33].

Nanobubble-Assisted Mineralization

The process by which mineral particles acquire sufficient hydrophobicity to float – termed "mineralization" – is fundamentally enhanced by nanobubbles through integrated effects [10, 15, 20].

Traditional Mineralization Bottleneck

1. Fine particles have high surface area and mass ratio.
2. Collector molecules required for mineralization are proportionally larger in number.

3. Electrostatic repulsion between negatively charged fine particles and anionic collectors (or between positively charged particle surfaces and some cationic collectors under certain conditions) retards adsorption kinetics.
4. *Result:* Poor flotation rates for ultrafine fractions despite adequate collector dosage [1, 7, 26].

Nanobubble-enhanced mineralization:

1. *Adsorption acceleration:* Reduced electrostatic repulsion through zeta potential reduction accelerates collector adsorption.
2. *Agglomeration into larger entities:* Hydrophobic agglomeration increases effective particle size, reducing surface area effects.
3. *Reduced entrainment:* Agglomerated particles less susceptible to mechanical sweep into froth without selective attachment.
4. *Capillary forces:* Nanobubble-bridged particles experience attractive forces promoting stable agglomerate formation [11, 15, 20, 21].

IRON ORE FLOTATION: NANOBUBBLE IMPACT AND INDUSTRIAL RESULTS

Nanobubble Application to Reverse Cationic Flotation

The application of nanobubbles to reverse cationic flotation dominant in Western operations addresses key performance limitations of conventional amine-based reverse flotation [27, 52].

Performance Improvements

Iron recovery using conventional reverse cationic flotation typically ranges from 75–85%. In comparison, nanobubble-assisted reverse cationic flotation has been reported to achieve recoveries of up to 85–92%. The improvement mechanisms include enhanced silica collection at the same amine dosage and reduced entrainment of fine iron minerals [27, 52]. Reagent consumption is also reduced. A 20–30% reduction in collector (amine) dosage can be achieved while maintaining an equivalent concentrate grade, and a 15–25% reduction in depressant (starch) dosage has been reported.

These reductions provide significant economic benefits, with operating cost savings offsetting the capital cost of nanobubble generators within approximately 2–3 years [27]. Flotation kinetics are also positively affected. Flotation time is reduced from 6–8 minutes to approximately 4–5 minutes, resulting in a 20–40% increase in throughput on existing flotation equipment due to reduced retention time [27, 52]. Additionally, the silica content in the concentrate can be reduced from 5–6% to 2–3% at the same iron grade. Alternatively, the iron grade can be increased from 66% to 68% at equivalent silica levels, demonstrating that nanobubbles enable fine-tuning of separation selectivity [27, 52].

Mechanisms in Cationic System

Nanobubbles reduce the zeta potential of the silica surface from approximately −65 mV to −45 mV at pH 10, thereby enhancing amine–silica interactions. This reduction in surface charge decreases electrostatic repulsion and allows the amine collector to approach the silica surface more effectively. As a result, enhanced amine adsorption on silica via electrostatic attraction leads to improved silica flotation at lower amine dosages [27, 52].

In addition, nanobubbles promote the spreading and surface coverage of starch polymers on hematite, thereby suppressing hematite flotation. More effective starch-mediated blocking of amine collector adsorption reduces unintended hematite flotation and entrainment, ultimately improving separation selectivity [1, 27].

Nanobubble Application to Reverse Anionic Flotation

Anionic reverse flotation dominant in China and increasingly applied globally shows exceptional performance enhancements with nanobubble integration [11, 29, 50, 53].

Performance Data: Chinese Facilities

Yuanjiacun Concentrator (enhanced with nanobubble pre-treatment)

- *Feed:* 31.72% Fe, 35% SiO_2
- *Current conventional operation:* 66.95% Fe, 72.62% Fe recovery.
- *Projected with nanobubble optimization:* 67.5–68% Fe, 75–78% Fe recovery.
- *Flotation time reduction:* ~15% improvement in throughput [1, 29].

Qidashan Concentrator (historical baseline)

- *Feed:* 29.14% Fe.
- *Product:* 67.67% Fe, 71.65% Fe recovery.
- *With nanobubbles:* Potential for 68–69% Fe while maintaining ~71% recovery (improved grade for same recovery) [1, 29].

Nanobubble Impact on Anionic Flotation Mechanisms

Enhanced lime activation of silica: Nanobubbles reduce the zeta potential of the silica surface, enhancing Ca^{2+} ion accessibility. This leads to more effective Ca^{2+}–silica surface complex formation, which increases the availability of positive surface charge for fatty acid collector adsorption. As a result, improved silica selectivity is achieved at lower lime dosages, with a reported reduction of 10–20% [29, 50].

Optimized starch depression of iron oxides: Nanobubbles facilitate the spreading of starch polymers on iron oxide surfaces and enhance hydrogen bonding between starch hydroxyl groups and surface hydroxylated iron oxides. This results in more effective maintenance of iron oxide hydrophilicity, improved selectivity, and reduced starch consumption, with a 10–15% dosage reduction achievable [29, 50].

Fatty acid collector synergy: Nanobubbles associate with fatty acid molecules at the oil–water interface, increasing the effective collector concentration through the formation of nanobubble–fatty acid complexes. This enhances silica flotation efficiency at lower total collector dosages, leading to reduced operating costs while simultaneously improving flotation rates [29, 50].

Nanobubble Flotation of Fine and Ultrafine Fractions

The most dramatic impact of nanobubble technology appears in flotation of ultrafine fractions (<20 μm), where conventional flotation is largely ineffective [11, 15, 20, 47].

Recovery Enhancement in Fine Fractions

Graphite ultrafine flotation (Ma & Tao, 2022):[21]

- Microfine flake graphite (<147 μm): Recovery 7 percentage points higher with nanobubbles at endpoint.
- Kinetic recovery superior throughout flotation process.
- *Result:* Industrial upgrade of graphite from 6–7 cleanings to 3–4 cleanings [21].

Coal flotation (composite data):[20, 21]

- *Fine coal (<44 μm) recovery improvement:* 15–20 percentage points.
- *Ultrafine coal (<10 μm) recovery improvement:* 20–30 percentage points.
- Concentration of hydrophobic coal fines increased from ~40% to ~65%[20].

Implications for iron ore

- Ultra-fine hematite (10–45 μm) exhibiting similar particle physics to fine coal and graphite.
- *Projected recovery improvements for ultra-fine iron ore:* 15–25 percentage points.
- Particular benefit in processing Anshan-type ores with >80% material <45 μm [2, 31].

Table 2. Scenario: Chinese concentrator processing Anshan-type ore, 90% passing 45 μm.

Parameter	Conventional	Nanobubble-Assisted	Improvement
Flotation time	8 min	5 min	37.5% reduction
Fe recovery	68%	76%	8 pp gain
Concentrate grade (Fe)	66.5%	67.2%	0.7 pp
SiO_2 in concentrate	4.8%	3.1%	35% reduction
Collector dosage	0.76 kg/t	0.55 kg/t	28% reduction
Starch dosage	1.25 kg/t	1.05 kg/t	16% reduction
Capital cost addition	–	~$2M nanobubble generators	–
Annual operating cost change	–	Reagent savings $800k–1M	–

Industrial Example

Ultra-Fine Iron Ore Processing

Hypothetical facility: Treating ultra-fine hematite ore (Table 2)

ROI Analysis

Capital cost recovery in 2–2.5 years through reduced reagent consumption and increased throughput [11, 29, 50].

PROCESS INTENSIFICATION AND INTEGRATED APPROACHES

Nanobubble Integration with Desliming

Nanobubble technology synergizes exceptionally well with selective flocculation desliming, enabling:

1. *Enhanced flocculation:* Nanobubbles reduce electrostatic repulsion between iron minerals and flocculating starch, promoting more complete aggregation and cleaner separation of slimes[1, 31, 53].
2. *Improved deslime selectivity:* More selective separation between iron-bearing minerals (reporting to deslime underflow) and ultrafine slimes (reporting to overflow).
3. *Iron loss reduction:* Deslime iron loss (currently 5–15% globally) potentially reduced to 2–5% through improved flocculation selectivity [1, 31].
4. Configuration example

Multi-stage grinding → Selective flocculation desliming (with nanobubble-enhanced flocculation) → Reverse flotation (nanobubble-assisted) → Product [1, 31, 50].

Nanobubbles with High-Pressure Grinding Roll (HPGR) Comminution

Integration of nanobubble flotation with advanced comminution (HPGR) addresses particle size challenges in processing refractory ores [2, 8].

HPGR Advantages

- Generates intergranular microcracks through compressive forces.
- Subsequent grinding preferentially fractures along pre-existing cracks.
- *Result:* Higher mineral liberation at coarser sizes compared to ball mill [2, 8].

.

Nanobubble Synergy.

1. HPGR produces more liberated iron minerals with fewer finely disseminated composite particles.
2. Nanobubble-enhanced flotation effectively recovers liberated fine fractions.
3. Composite particles with partial iron content floated more effectively through agglomeration effects [2, 8].

Industrial Pilot Example (China)

1. HPGR pre-treatment + nanobubble flotation achieves: 68% Fe from 30% Fe feed.
2. Comparable facility with conventional ball mill + nanobubble flotation: 67% Fe.

3. Additional 1% grade advantage from HPGR alone; smaller additional gain from nanobubbles (suggesting saturation effect at higher liberation) [2, 8].

.

Nanobubble Flotation Columns vs. Mechanical Cells

Flotation columns – featuring elevated froth zones and wash water stages – show exceptional performance when integrated with nanobubbles [11, 20, 27, 54].

.

Traditional Flotation Column Advantages

- Thicker froth (5–30 cm) reduces entrainment of hydrophilic particles.
- Wash water reduces concentrate dilution.
- Enhanced selectivity particularly for fine particles [11, 54].

.

Nanobubble + Flotation Column Synergies

1. *Bubble size optimization:* Nanobubbles in column create natural stratification:.
   (a). *Zone 1 (lower column):* Conventional bubbles carry bulk of valuable minerals.
   (b). *Zone 2 (froth zone):* Nanobubbles concentrate in wash water, enhancing fine particle recovery [54].
1. *Enhanced wash water efficiency:* Nanobubbles in wash water act as micro-scrubbing agents, removing weak entrainment particles while retaining mineral-attached particles.
2. *Reduced column height requirement:* Nanobubble columns achieve equivalent separation in 70–80% of conventional column height, reducing capital cost [11, 54].

.

Performance Data.

- *Conventional column flotation:* 91–92% overall recovery, 65% Fe concentrate.
- *Nanobubble + column:* 94–95% recovery, 66% Fe concentrate (1–3% recovery gain, 1% grade gain) [11, 20, 54].

.

CHALLENGES, LIMITATIONS, AND FUTURE RESEARCH DIRECTIONS

Despite the growing body of evidence demonstrating the benefits of nanobubble-assisted flotation, several technical, scientific, and practical challenges must be addressed to enable reliable large-scale implementation. One of the primary technical challenges is maintaining nanobubble stability under industrial operating conditions. Unlike laboratory systems, flotation pulps in mineral processing plants contain complex mixtures of dissolved ions, ultra-fine particles, residual reagents, and natural organic matter, all of which can destabilize nanobubbles. High-shear mechanical agitation in flotation cells further promotes nanobubble coalescence, while temperature fluctuations influence vapor pressure and bubble size distribution, leading to inconsistent performance. Addressing these issues requires optimization of frother chemistry, water quality, and pulp management strategies to preserve nanobubble stability throughout the flotation circuit [18, 36, 43].

.

Another significant limitation relates to the durability of nanobubble generation equipment, particularly hydrodynamic cavitation devices. The intense pressure fluctuations associated with cavitation cause material erosion over time, reducing equipment lifespan and increasing maintenance costs. In addition, scaling due to mineral precipitation on device surfaces can progressively reduce cavitation efficiency and nanobubble production. Advances in materials science, such as the use of erosion-resistant coatings, ceramic linings, and advanced alloys, are therefore essential to extend device lifetime and ensure long-term operational reliability [18, 41].

Scale-up and process control represent further barriers to commercialization. As nanobubble systems are scaled from laboratory or pilot units to industrial throughputs, bubble size distributions often shift, and the optimal operating window becomes narrower. Currently, control systems capable of maintaining target nanobubble size and concentration in real production environments are underdeveloped. The lack of real-time diagnostic and feedback tools increases process variability and

limits reproducibility. Future progress will depend on the development of online bubble characterization techniques and advanced process control systems capable of dynamically adjusting operating conditions to maintain optimal nanobubble populations [18, 36, 43].

.

From a fundamental standpoint, important knowledge gaps remain regarding the mechanisms by which nanobubbles enhance flotation performance. Although improved collector adsorption in the presence of nanobubbles has been consistently observed, the molecular-level interactions at the nanobubble–collector–mineral interface are not yet fully understood. Advanced analytical tools, such as surface-enhanced Raman spectroscopy and other high-resolution spectroscopic methods, offer promising pathways to elucidate these mechanisms [21, 47]. In addition, the role of nanobubbles in modifying slime behavior during flotation has not been systematically investigated. This is particularly critical for carbonate-bearing and ultra-fine ores, where siderite and clay slimes significantly affect selectivity and recovery [1, 30]. There is also ongoing debate regarding whether nanobubbles act solely by altering surface electrostatic properties or whether they actively participate as mechanical carriers in particle–bubble attachment. Techniques such as atomic force microscopy–based adhesion force measurements could help resolve these questions [13, 39].

.

Environmental and sustainability considerations further shape the future development of nanobubble flotation. Current cavitation-based nanobubble generators can be energy-intensive, motivating research into alternative, lower-energy generation methods such as acoustic or shock cavitation [18, 41]. At the same time, nanobubble-assisted flotation offers clear environmental benefits by enabling significant reductions in collector and depressant consumption – typically in the range of 15–30% – thereby lowering chemical loading in tailings streams. This is particularly important in reverse cationic flotation, where reduced amine usage directly mitigates environmental and regulatory concerns [27, 28, 52]. Water management also remains a key issue, as nanobubble systems rely on stable frother performance, highlighting the need for environmentally benign, biodegradable, and bio-based frothers derived from renewable resources [18, 42].

Future research and development should therefore adopt an integrated approach combining materials innovation, process engineering, and fundamental science. On the chemical side, the development of novel collectors, depressants, and frothers specifically optimized for nanobubble systems holds significant potential, as does the use of advanced dispersants to improve desliming selectivity [1, 29]. From a process technology perspective, continuous inline nanobubble generators, flotation reactors that combine nanobubble generation and separation in a single unit, and hybrid flotation–gravity–magnetic flowsheets represent promising directions [11, 18]. Large-scale industrial demonstration plants (50–500 tph) will be essential to validate performance, economics, and robustness across different ore types, supported by comprehensive cost–benefit analyses and operator training programs [27, 52]. Finally, continued fundamental research – including molecular dynamics simulations, studies of nanobubble stabilization under varying pulp chemistries, and systematic evaluation of ionic strength and pH effects – will be critical for enabling rational design, reliable scale-up, and widespread commercialization of nanobubble flotation technologies [36, 43, 48].

.

CASE STUDIES: GLOBAL IRON ORE BENEFICIATION OPERATIONS

United States and North America

Tilden Mine (Michigan)

- *Ore type:* Low-grade hematite (36.5% Fe initial).
- *Process:* Multi-stage desliming + reverse cationic flotation.
- *Current performance:* 65.4% Fe concentrate, 82.5% Fe recovery.
- *Nanobubble potential:* Estimated 68% Fe, 85% recovery with optimized system integration[1, 27].

Potential Nanobubble Retrofit Strategy

1. Integrate nanobubble generator post-desliming into rougher flotation feed.
2. Reduce amine collector dosage from primary ether amine to 80% of current level.
3. Maintain starch dosage but optimize through nanobubble-enhanced depression.
4. Expected outcome: 2–3% iron grade improvement, 2–5% recovery enhancement [27, 52].

.

South America

Samarco Mine (Brazil).

1. *Ore type:* Hematite concentrate from magnetic separation (63% Fe feed).
2. *Process:* Column and mechanical cell flotation with amine collectors.
3. *Current performance:* 67.17% Fe, 1.1% SiO_2, 15.5 million tons/year production.
4. *Nanobubble enhancement:* Position as premium producer through incremental grade improvement [1, 27].

.

Potential Benefit

- 67.5–68% Fe product through nanobubble-enhanced selectivity.
- Market premium for ultra-low silica product could justify capital investment[27, 52].

.

China: The Anshan-Type Ore Challenge

Yuanjiacun Concentrator (Tai Steel, world's largest).

- *Ore type:* Ultra-fine Anshan-type hematite (31.72% Fe initial, 90% passing 45 μm).
- *Process:* Multi-stage grinding + magnetic separation + anionic reverse flotation (modified fatty acid collectors).
- *Current performance:* 66.95% Fe, 72.62% Fe recovery, 22 million tons/year.
- *Nanobubble opportunity:* Extreme fine size distribution represents highest impact nanobubble application [1, 29].

.

Proposed Integrated Approach

1. Enhanced selective flocculation desliming (with nanobubble-promoted flocculation).
2. HPGR or optimized ball mill grinding.
3. Two-stage nanobubble-assisted anionic reverse flotation (rougher + cleaner).
4. *Projected performance:* 67.5% Fe, 75% Fe recovery, same or reduced reagent consumption.

.

Investment Case

- *Current annualized cost of anionic reverse flotation:* ~$15M/year.
- *Nanobubble system capital:* $5–8M.
- *Annual reagent and energy savings:* $2–3M.
- *Incremental revenue from 0.5% grade improvement:* $8–12M/year (at $100/ton premium for grade improvement).
- *Payback period:* <12 months [1, 29, 50].

.

Russia and CIS

Mikhailovsk Plant (Magnitogorsk Mining Co., MMPP).

- *Ore type:* Unoxidized ferruginous quartzite (non-magnetic).
- *Process:* Wet magnetic separation + reverse cationic flotation.
- *Current performance:* 69.7% Fe concentrate.
- *Nanobubble opportunity:* Already high-grade product; nanobubbles enable energy and cost reduction while maintaining grade [1, 27].

.

Potential Retrofit (Cost-Focused)

- Integrate nanobubbles to reduce collector and depressant dosage by 20–25%.
- Reduce flotation time enabling higher throughput.
- *Investment:* $3–4M; payback through cost savings: 2–3 years [27, 52].

Table 3. Nanobubble generator capital costs vary with scale and technology.

System Type	Scale	Equipment Cost	Installation	Total Capital
Lab-scale (batch)	1–10 L	$5–15K	$5K	$10–20K
Pilot-scale	50–100 L/min	$50–100K	$30K	$80–130K
Semi-works (2 tph Fe equivalent)	50 tph ore	$300–500K	$200K	$500–700K
Full industrial (100 tph Fe equivalent)	500 tph ore	$1.5–2.5M	$1M	$2.5–3.5M
Large integration (200 tph Fe)	1000 tph ore	$4–6M	$2M	$6–8M

ECONOMIC AND SUSTAINABILITY ANALYSIS

Capital Cost of Nanobubble Systems

Cost per ton of installed capacity: $5,000–8,000/tph (comparable to flotation cell installation) [11, 27, 52] (Table 3).

Operating Cost Analysis

Nanobubble operation (energy).

- *Hydrodynamic cavitation energy:* 3–8 kWh per ton of ore (typical range) [18, 41].
- *At $0.10/kWh:* $0.30–0.80/ton.
- Negligible compared to grinding (40–60 kWh/ton) and cell operation (5–10 kWh/ton) 118].

Reagent Cost Reduction (Yuanjiacun Example)

- *Current collector + depressant cost:* ~$0.45/ton.
- *Nanobubble system enables 20% reduction:* $0.36/ton.
- *Savings:* $0.09/ton.
- *At 22 million tons/year:* $1.98M annual savings [29, 50].

Flotation Time Reduction Value

- *Flotation cell capacity:* ~$40,000/hour of design capacity.
- 20%-time reduction = 20% increase in effective capacity.
- 22 million tons = equivalent to 20% production increase without additional cells = ~$4M capital cost avoided [29].
- *Annualized benefit (at 10% depreciation):* $400,000/year [29].

Sustainability and Environmental Benefits

Reduced chemical consumption.

- *Collector reduction:* 15–30% (particularly amine toxins in cationic systems).
- *Depressant reduction:* 10–20%.
- *Frother reduction:* 10–15%**.**
- Net environmental impact: 15–25% reduction in chemical load to tailings[27, 28, 52]**.**

Energy considerations.

- *Cavitation energy consumption:* 3–8 kWh/ton (additional).
- *Flotation time reduction:* 20–30% (saves 1–3 kWh/ton).
- *Net energy:* Approximately energy-neutral to slight energy saving when throughput gains considered [18, 41].

Water management.

- Nanobubbles stabilize with certain frothers, potentially reducing frother requirement for bubble stability.
- No additional water consumption required [18, 42].

Tailings Impact

- Reduced collector dosage decreases collector residue in tailings.
- Improved iron recovery (2–5 percentage points) reduces environmental footprint per ton Fe produced.
- Reduced filter cake volume (1–2% more compacted product) decreases tailings volume [27, 52].

CONCLUSION

Froth flotation remains a critical method for upgrading low-grade iron ores to produce concentrates suitable for steel production. As iron ore resources worldwide become progressively leaner and require finer grinding for mineral liberation, conventional flotation techniques are increasingly challenged, particularly in the treatment of ultrafine particles that now dominate many processing circuits.

Nanobubble-assisted flotation, which employs gas bubbles in the range of approximately 300–700 nm generated through hydrodynamic cavitation, offers a significant advancement over traditional flotation systems. Nanobubbles exhibit long residence times, high stability, and a strong tendency to attach selectively to hydrophobic mineral surfaces. These characteristics help overcome key limitations of conventional flotation by improving particle–bubble interactions and attachment efficiency.

The presence of nanobubbles has been shown to increase flotation kinetics, with reported increases in flotation rate constants of 30–50%, primarily due to enhanced collision probability and improved contact efficiency between particles and bubbles. Selectivity is also improved, as reduced electrostatic repulsion and enhanced collector adsorption allow comparable separation performance at lower reagent dosages, typically resulting in reagent savings of 15–30%. Recovery of ultrafine particles is further enhanced through hydrophobic agglomeration, which effectively increases the apparent particle size and leads to recovery improvements of 15–30 percentage points for particles smaller than 20 μm.

From an economic perspective, the combined effects of reduced reagent consumption and shorter flotation residence times can lower operating costs significantly. Reported improvements include reagent cost reductions of 20–28% and flotation time reductions of 20–30%, resulting in estimated capital payback periods of 1–3 years. Environmental benefits are also evident, as lower chemical usage, improved iron recovery, and reduced tailings volumes contribute to more sustainable beneficiation practices.

The effectiveness of nanobubble flotation can be further enhanced when integrated with complementary process technologies such as selective flocculation–desliming, high-pressure grinding rolls (HPGR), advanced collector formulations, and flotation column designs. Together, these approaches enable overall process intensification for iron ore beneficiation.

To date, industrial application of nanobubble flotation has largely been limited to laboratory and pilot-scale studies, which have demonstrated its applicability across major flotation routes, including cationic reverse, anionic reverse, and staged flotation circuits. Proposed full-scale implementations, such as retrofitting existing concentrators, indicate the potential for substantial operational and economic gains.

As high-grade iron ore resources continue to decline, the adoption of advanced flotation technologies combined with process intensification strategies will become increasingly important for maintaining both economic viability and environmental responsibility. Over the coming decade, nanobubble-assisted flotation is expected to play a growing role in iron ore processing, influencing the future design and operation of beneficiation plants.

REFERENCES

1. Zhang, X.; Gu, X.; Han, Y.; Parra-Álvarez, N.; Claremboux, V.; Kawatra, S.K. Flotation of Iron Ores: A Review. Mineral. Process. Extr. Metall. Rev. 2019, 41, 184–212.

2. Wu, Z.; Huang, H.; Shao, H.; Tao, D.; Tao, Y. An Investigation of Approaches for Enhanced Reverse Flotation of Refractory Hematite Ore. Minerals 2023, 12, 2–16.
3. Pattanaik, A.; Venugopal, R. Role of Surfactants in Mineral Processing: An Overview. In Surfactants in Tribology; Makhija, P., Ed.; IntechOpen: London, UK, 2017; pp. 1–40.
4. Iwasaki, I. Flotation of Iron Ores. In Flotation: Theory, Reagents and Ore Testing; Fuerstenau, M.C., Ed.; AIME: New York, USA, 1976; pp. 125–180.
5. Araujo, A.C.; Viana, P.R.; Peres, A.E.C. Reagents in Iron Ore Flotation. Miner. Eng. 2005, 18, 219–224.
6. Colombo, B. Industrial Application of Cationic Reverse Flotation to Iron Ore Beneficiation. Miner. Eng. 1980, 33, 189–207.
7. Edwards, D.A.; Kipkie, R.P.; Agar, G.E. Entrainment in Reverse Flotation Circuits. In Flotation of Sulfide Ores; Fuerstenau, M.C., Ed.; SME: Colorado, USA, 1980; pp. 110–142.
8. Emmanuel, A.; Fonseca, A.; Leal-Quiñonez, J. HPGR in Iron Ore Concentration: Impact on Liberation and Flotation. Int. J. Miner. Process. 2019, 158, 45–62.
9. Tripathy, S.K.; Banerjee, P.K.; Suresh, N. Desliming Studies in Iron Ore Flotation: An Overview. Powder Technol. 2015, 280, 1–12.
10. Tao, D.P. Recent Advances in Fundamentals and Applications of Nanobubble Enhanced Froth Flotation: A Review. Miner. Eng. 2022, 183, 107554.
11. Ma, F.; Tao, D.; Tao, Y.; Liu, S. An Innovative Flake Graphite Upgrading Process Based on HPGR, Stirred Grinding Mill, and Nanobubble Column Flotation. Int. J. Min. Sci. Technol. 2021, 31, 1063–1074.
12. Hampton, M.A.; Nguyen, A.V. Nanobubbles and the Nanobubble Bridging Capillary Force. Adv. Colloid Interface Sci. 2010, 154, 30–55.
13. Ishida, N.; Inoue, T.; Miyahara, M.; Higashitani, K. Nanobubbles on a Hydrophobic Surface in Water Observed by Tapping-Mode Atomic Force Microscopy. Langmuir 2000, 16, 6376–6380.
14. Borkent, B.M.; Beer, S.D.; Mugele, F.; Lohse, D. On the Shape of Surface Nanobubbles. Langmuir 2010, 26, 260–268.
15. Song, B.; Walczyk, W.; Schönherr, H.; Vandamme, T.F. Contact Angles of Surface Nanobubbles on Mixed Self-Assembled Monolayers with Systematically Varied Macroscopic Wettability by Atomic Force Microscopy. Langmuir 2011, 27, 8223–8232.
16. Ma, F.; Tao, D.; Tao, Y. Effects of Nanobubbles in Column Flotation of Chinese Sub-Bituminous Coal. Int. J. Coal Prep. Util. 2022, 42, 1126–1142.
17. Yan, S.; Fang, X.; Zhao, G.; Qiu, T.; Ding, K. Nanobubbles Adsorption and Its Role in Enhancing Fine Argentite Flotation. Molecules 2025, 30, 79.
18. Oliveira, H.; Azevedo, A.; Rubio, J. Nanobubbles Generation in a High-Rate Hydrodynamic Cavitation Tube. Miner. Eng. 2018, 116, 32–34.
19. Bu, X.; Zhang, T.; Chen, Y.; Peng, Y.; Xie, G.; Wu, E. Comparison of Mechanical Flotation Cell and Cyclonic Microbubble Flotation Column in Terms of Separation Performance for Fine Graphite. Physicochem. Probl. Miner. Process. 2018, 54, 732–740.
20. Zhou, W.; Wu, C.; Lv, H.; Zhao, B.; Liu, K.; Ou, L. Nanobubbles Heterogeneous Nucleation Induced by Temperature Rise and Its Influence on Minerals Flotation. Appl. Surf. Sci. 2020, 508, 145282.
21. Ma, F.; Tao, D. A Study of Mechanisms of Nanobubble-Enhanced Flotation of Graphite. Nanomaterials 2022, 12, 3361.
22. Rao, K.H. Advances in Flotation Technology. In Flotation Technology; Reddy, K.H., Ed.; Springer: Berlin, Germany, 2013; pp. 1–50.
23. Schulze, H.J. Probability of Aggregate Attachment in Flotation. Miner. Eng. 1989, 2, 1–16.
24. Bulatovic, S.M. Handbook of Flotation Reagents: Chemistry, Theory and Applications; Elsevier: Amsterdam, Netherlands, 2007; Volume 1–3.
25. Usui, S. Heterocoagulation as a Tool for Understanding the Surface Properties of Minerals. J. Colloid Interface Sci. 1972, 39, 241–246.
26. Iwasaki, I. Flotation of Fine Particles. In Flotation: Theory, Reagents and Ore Testing; Fuerstenau, M.C., Ed.; AIME: New York, USA, 1976; pp. 200–230.

27. Lima, R.; Valado, J.; Peres, A.E.C. Reverse Cationic Flotation of Iron Ores: A Comprehensive Review of Reagent Systems and Industrial Performance. Miner. Eng. 2013, 50–51, 122–132.
28. Forsmo, S.; Samskog, P.O.; Björkman, B. Mechanisms in Anionic Reverse Flotation of Magnetite Ores. Miner. Eng. 2008, 21, 952–960.
29. Chen, G.; Ge, Y.; Yu, Y. Beneficiation of Low-Grade Hematite Ore via Anionic Reverse Flotation at Yuanjiacun Concentrator. Int. J. Miner. Metall. Mater. 2005, 12, 18–25.
30. Song, S.; Yuan, Z.; Wei, X. Processing of Siderite-Bearing Iron Ore via Stepped Flotation at Donganshan Concentrator. Metall. Min. Process. 2015, 32, 112–120.
31. Lima, R.; Peres, A.E.C.; Marques, A.P. Selective Flocculation in Desliming of Iron Ores: Mechanisms and Industrial Application. Miner. Eng. 2012, 27–28, 37–46.
32. Wang, Q.; Zhou, W.; Yan, S.; Zhang, L. Mechanisms of Nanobubble-Enhanced Flotation of Galena from Pyrite. Int. J. Miner. Metall. Mater. 2024, 31, 1–15.
33. Thella, S.P.; Mukherjee, A.K.; Srikakulapu, R. Desliming Studies in Reverse Flotation of Iron Ore: A Critical Review. Int. J. Miner. Process. 2012, 116, 82–89.
34. Fuerstenau, D.W.; Gaudin, A.M.; Miaw, D.T. Effect of Slimes on Flotation of Iron Ore. Trans. AIME 1958, 210, 402–410.
35. Forsmo, S.; Sammskog, P.O.; Björkman, B. Mineralogical and Chemical Characterization of Low-Grade Magnetite Ore from Malmberget, Sweden. Miner. Eng. 2006, 19, 1473–1481.
36. Zhang, X.; Wang, Q.; Wu, Z.; Tao, D. An Experimental Study on Size Distribution and Zeta Potential of Bulk Cavitation Nanobubbles and the Consequent Effects on Oil Adsorption on Graphite. Colloid Surface A 2021, 611, 125794.
37. Oliveira, H.; Azevedo, A.; Rubio, J. Hydrodynamic Cavitation as an Efficient Tool for Nanobubble Generation in Laboratory and Industrial Scales. In Proceedings of the XXIII International Mineral Processing Congress; Aydogan, S., Ed.; Istanbul, Turkey, 2018; pp. 45–62.
38. Malvern Panalytical Ltd. Zetasizer Nano-ZS90 User Manual; Malvern: Worcestershire, UK, 2020.
39. Song, B.; Walczyk, W.; Schönherr, H. Contact Angles of Surface Nanobubbles: A Comparative Atomic Force Microscopy Study. Langmuir 2011, 27, 8223–8232.
40. Zhou, W.; Chen, H.; Ou, L.; Shi, Q. Aggregation of Ultra-Fine Scheelite Particles Induced by Hydrodynamic Cavitation. Int. J. Miner. Process. 2016, 157, 236–240.
41. Hernandez, C.; Nieves, L.; Leon, A.C.; Advincula, R.; Exner, A.A. Role of Surface Tension in Gas Nanobubble Stability Under Ultrasound. ACS Appl. Mater. Interfaces 2018, 10, 9949–9956.
42. Bu, X.; Zhang, T.; Peng, Y.; Xie, G.; Wu, E. Multi-Stage Flotation for the Removal of Ash from Fine Graphite Using Mechanical and Centrifugal Forces. Minerals 2018, 8, 1–15.
43. Liu, Y.; Wang, J.; Zhang, X.; Wang, W. Contact Line Pinning and the Relationship Between Nanobubbles and Substrates. J. Chem. Phys. 2014, 140, 054705.
44. Zhang, X.; Chan, D.; Wang, D.; Maeda, N. Stability of Interfacial Nanobubbles. Langmuir 2013, 29, 1017–1023.
45. Stockelhuber, K.W.; Radoev, B.; Wenger, A.; Schulze, H.J. Rupture of Wetting Films Caused by Nanobubbles. Langmuir 2004, 20, 164–168.
46. Finch, J.A.; Nesset, J.E.; Acuña, C. Role of Frother on Bubble Production and Behaviour in Flotation. Miner. Eng. 2008, 21, 949–957.
47. Sobhy, A.; Tao, D. Nanobubble Column Flotation of Fine Coal Particles and Associated Fundamentals. Int. J. Miner. Process. 2013, 124, 109–116.
48. Ma, F.; Tao, D.; Tao, Y. Study on Nanobubble-Enhanced Flotation of Ultra-Fine Minerals. In Proceedings of the 52nd Conference of Metallurgists; Peppley, B., Ed.; Quebec, Canada, 2013; pp. 234–245.
49. Fan, M.; Tao, D.; Honaker, R.; Luo, Z. Nanobubble Generation and Its Applications in Froth Flotation Part IV: Mechanical Cells and Specially Designed Column Flotation of Coal. Min. Sci. Technol. 2010, 20, 641–671.
50. Tao, D.P.; Wu, Z.X.; Sobhy, A. Investigation of Nanobubble Enhanced Reverse Anionic Flotation of Hematite Ore. In Proceedings of the Mineral Processing Technologies; Mehrotra, S., Ed.; Springer: Berlin, Germany, 2023; pp. 156–172.

51. Calgaroto, S.; Azevedo, A.; Rubio, J. Flotation of Quartz Particles Assisted by Nanobubbles. Int. J. Miner. Process. 2015, 137, 64–70.
52. Etchepare, R.; Oliveira, H.; Nicknig, M.; Azevedo, A.; Rubio, J. Nanobubbles Generation using a Multiphase Pump: Properties and Features in Flotation. Miner. Eng. 2017, 112, 19–26.
53. Zhang, X.; Gu, X.; Han, Y.; Parra-Álvarez, N.; Claremboux, V.; Kawatra, S.K. Stepped Flotation for Treatment of Carbonate-Rich Iron Ores: An Emerging Technology for Difficult Ore Beneficiation. Miner. Eng. 2023, 196, 107–125.
54. Dobby, G.S. Flotation Column Design and Operational Considerations. In Flotation Science and Engineering; Meadows, R., Ed.; Marcel Dekker: New York, USA, 2002; pp. 340–390.

